Design, Acceptance and Capacity of Subsea Open Cables

Elizabeth Rivera Hartling, Alexei Pilipetskii, *Fellow, IEEE*, Darwin Evans, Eduardo Mateo, Massimiliano Salsi, Pascal Pecci, and Priyanth Mehta

(Tutorial)

***Abstract*—This article will discuss the collaboratively formed cross-industry open cables concept for characterizing optical performance of undersea cables with the intent of assessing and understanding their capacity potential. The article proposes definitions of two critical nonlinear and linear performance metrics for open cables: GSNR (Gaussian or generalized signal to noise ratio) and $\mathrm{SNR_{ASE}}$ (Signal to noise ratio amplified spontaneous emission), including effects such as GAWBS (guided acoustic wave Brillouin scattering) and signal droop. Measurement methodologies for these metrics are proposed, with considerations for limitations and impact of the test conditions and characteristics of the transponders used. Expanded definitions are offered to enable variable symbol rate transponders to be used for measurement, with considerations for scaling of SNR values. Considerations for using these metrics for capacity assessment and applying these techniques to concatenated multi-segment systems are introduced. Recommendations on key parameters for system specification, system characterization, and proposals for SNR-based performance budgeting tables are also discussed as foundational elements to enabling accurate estimation of the capacity potential of a subsea open cable.**

***Index Terms*—Acceptance, budget table, capacity, concatenation, droop, GAWBS, GOSNR, GSNR, key parameter table open, open cable, optical network, OSNR, SNR, submarine, undersea.**

I. Introduction

SUBMARINE systems have undergone significant evolution in the past decade, with the advent of coherent technology and dispersion-uncompensated D+ cables. One of the important practical implications of dispersion-uncompensated transmission, in contrast to previous generations of systems using dispersion-managed transmission, is weak dependence between path design optimization and transponder type as well as modulation formats [1], [2]. Based on these properties, the Open Cables concept is introduced, which suggests that the optical transmission path can be designed, optimized and characterized independently of transponder technology. A system design can then allow a flexible choice of the transponders, provided certain performance requirements are met. The concept has sparked a broad industry shift towards Open Cables due to the significant benefits in capacity potential enabled by independent selection of best-of-breed wet plant and dry plant, in addition to extensive operational and economic benefits [3]–[6]. However, Open Cables have also necessitated a shift in the performance metrics and acceptance parameters historically used for subsea systems, which were traditionally tied exclusively to the capacity and Q margin of a specific transponder technology supplied by the wet plant vendor [7]. In this paper, we use Q to represent Q^2 factor, as is most commonly used in subsea applications.

This paper presents an industry-wide Open Cable effort to re-define the cable performance metrics such that they can be specified and measured independently of any one vendor's transponder technology. Early proposals for Open Cable performance metrics referenced linear OSNR (Optical Signal to Noise Ratio) and nonlinear GOSNR (Gaussian or Generalized Optical Signal to Noise Ratio) [6], [8]–[11]. At the time, approximately 30 to 35 Gbaud 100G DP-QPSK was the prevalent coherent technology used, and as such it was logical for GOSNR to be defined in reference to 120 channels and 37.5 GHz carrier spacing in a typical 4.5 THz-wide submarine C-band. 100G QPSK was also suggested as the instrument to measure and characterize cable performance using the inverse back-to-back method [8]. With the fast-paced evolution of coherent technology towards higher symbol rates, variable bitrates and probabilistic constellation shaping, GOSNR needs to be adapted to become the symbol rate, modulation format and channel spacing independent metric GSNR (Gaussian or Generalized Signal to Noise Ratio) [12]. Equally, these advancements in coherent technology have also quickly diminished the likelihood that early generation 30 to 35 Gbaud QPSK transponders will be maintained for years to come. This necessitates an expansion of previously proposed measurement recommendations in [12] to broaden the scope of applicable specifications for transponders to be used as GSNR measurement tools within the recommended methodologies,

Manuscript received July 31, 2020; revised November 12, 2020; accepted December 6, 2020. Date of publication December 16, 2020; date of current version February 2, 2021. *(Corresponding author: Elizabeth Rivera Hartling).*

Elizabeth Rivera Hartling is with Facebook Inc., Menlo Park, CA 94025 USA (e-mail: elizabethrh@fb.com).

Alexei Pilipetskii is with Subcom, Eatontown, NJ 07724 USA (e-mail: apilipetskii@subcom.com).

Darwin Evans and Priyanth Mehta are with Ciena Corporation, 385, Terry Fox Dr. Ottawa K2K 0L1, Canada (e-mail: daevans@ciena.com; prmehta@ciena.com).

Eduardo Mateo is with NEC Corporation., Tokyo 108-8001, Japan (e-mail: e-mateo@nec.com).

Massimiliano Salsi is with Google Inc., Mountain View, CA 94043 USA (e-mail: massimilianosalsi@gmail.com).

Pascal Pecci is with Alcatel Submarine Networks, 91620 Nozay, France (e-mail: pascal.pecci@asn.com).

Digital Object Identifier 10.1109/JLT.2020.3045389

where GSNR is a metric independent of symbol rate and channel count.

Design shifts in subsea cable optical designs towards high fiber count SDM (spatial division multiplexing) cables [13]–[18] and lower per fiber power as a result of optimization has also reduced the relative contribution of nonlinear noise to GSNR [19]. Thus, less variation in estimated cable capacity is expected when experimentally obtaining GSNR using different modulation schemes and symbol rates. The paper discusses in more details this aspect of the Open Cable characterization.

The paper focuses as well on other effects contributing to GSNR namely GAWBS [20] which became more pronounced due to the introduction of low loss D+ fibers in high bit rate coherent systems [21]–[24] and the effect of signal droop which needs to be accurately accounted for, especially in SDM cables with lower per fiber power [25].

Finally, the paper discusses and proposes SNR-based system design performance budgets, as well as methodologies to evaluate Open Cable capacity potential with a given transponder technology and as a Shannon channel.

II. Key Performance Metrics

In [12], the authors presented definitions for GSNR and $\mathrm{SNR_{TOT}}$. Here, we review these previous definitions and introduce key expansions and considerations.

In order to properly discuss the nuances of OSNR and GOSNR in relation to designing and characterizing Open Cables, we must first define each metric with consistency and clarity. This section will introduce the definitions, the variations that exist and what is included or excluded for each, such that the language used to describe these important concepts is well understood.

A. Previous Definition of (G)OSNR

In subsea optical transmission, OSNR describes the relative noise introduced by the repeaters along the subsea line, as a result of Amplified Spontaneous Emission (ASE), also known as $\mathrm{OSNR_{ASE}}$. OSNR is highly dependent on the conditions under which it is defined. There are several OSNR values that are often used in Open Cable designs, such as Design OSNR, Nominal OSNR and Commissioning OSNR.

It is important to note that OSNR, when defined in its most commonly used units of dB/0.1 nm, is highly dependent on the reference channel count. It is common (for historical reasons) to use 120 channels as a reference, however any channel count could be used, if it is consistently used. Otherwise, defining OSNR as a pure ratio in units of dB, also known as SNR (or $\mathrm{SNR_{ASE}}$), eliminates this potential area of confusion when dealing with variable symbol rates and channel counts, and is discussed in Section II-B.

OSNR varies over frequency across the available optical bandwidth. As such, using OSNR as an average value is helpful in simplifying discussions. A Worst Case OSNR, or the lower bound, of all the channels can also be defined.

The Design OSNR (average) is calculated using the classical formula [26]:

$$OSNR_{Design} = 58 + P_{TOP} - N_{Ch} - G - NF - N_R \quad \text{(average, per channel, in dB/0.1 nm)} \tag{1}$$

where,

58 is a constant related to the central wavelength of the spectrum

P_{TOP} is the EDFA Total Output Power (TOP) within the repeater in dBm

N_{Ch} is the number of channels in dB

G is the repeater gain in dB

NF is the noise figure of the repeater in dB

N_R is the number of repeaters in dB.

The Design OSNR is very simple to calculate based on high level system specifications but does not consider all the impairments that will be present in a practical system. As such, a second OSNR value is often quoted, called the Nominal OSNR (average). This OSNR is based on the Design OSNR, beyond which any path ROADM penalties are added, and the droop is considered (see II-D for more details on droop).

$$OSNR_{Nominal} = OSNR_{Design} - ROADM\ Penalties - Droop_{ASE}\ \text{(average, per channel, in dB/0.1 nm)} \tag{2}$$

Under ideal conditions, $OSNR_{Nominal}$ should represent a field measurable quantity. However, due to real-world non-idealities and variations, some additional margins are generally considered. These margins account for effects such as variations from expectations in fiber loss, or variability in repeater TOP from nominal, as examples. As a consequence, a Commissioning OSNR is defined. System acceptance is then defined around the specified Commissioning OSNRs, typically considering average and worst case.

$$OSNR_{Commissioning} = OSNR_{Nominal} - Supplier\ Margin \quad \text{(average, per channel, in dB/0.1 nm)} \tag{3}$$

Finally, the Worst Case Commissioning OSNR is also defined. During commissioning and acceptance, each channel individually should be above this Worst Case $OSNR_{Commissioning}$.

In addition to OSNR, a second performance metric has been defined almost 10 years ago in [1], [2].

The concept that leads to the GOSNR is the fact that for uncompensated optical transmission nonlinearities (NLI) can be considered as an additive white Gaussian noise (AWGN) statistically independent of ASE noise. As a consequence, the following formula has been defined:

$$\frac{1}{GOSNR} = \frac{1}{OSNR_{ASE}} + \frac{1}{OSNR_{NLI}} \tag{4}$$

where $OSNR_{NLI}$ is the noise coming from nonlinearities.

In the last years, the Gaussian Noise (GN) model evolved with extended version and also other phenomena have been added. In the following paragraphs, OSNR/GOSNR will be converted into SNR/GSNR, and GAWBS and droop will be considered in our expanded definitions in Section II-C and II-D.

B. SNR Scaling in Submarine Systems

Subsea optical amplifiers, called repeaters in a submarine cable system, operate at constant pump power, unlike the terrestrial amplifiers which are typically operated at constant gain. The TOP of subsea repeaters is virtually unchanged when the number of channels, or more generally the power profile, in the system changes. This unique characteristic allows for the

common practice of simple scaling of specific OSNR measurements to different channel counts, within reasonable bounds. For example, if OSNR is measured as dB/0.1nm with 45 channels but is desired to be reported in dB/0.1 nm for 120 channels, then the delta between the measured data and the desired value is $10 \times \log_{10}(45/120) = -4.26$ dB. The reason is that the larger number of channels will share the same total power and as a consequence the signal power will be lower, without notably impacting the underlying noise floor measurement.

There are underlying assumptions in this scaling that the power spectral density (PSD) is not meaningfully different under the different channel counts, that a uniform channel spacing is used, and that all spectral power has been fully accounted for in the baseline measurement. For example, scaling OSNR between 2 channels and 120 channels would not be meaningful, as the effects of spectral hole burning and an uneven PSD in the 2-channel case would introduce significant error.

In this paper, and in [12], $GSNR$ and SNR_{ASE} are defined as metrics that are independent of channel spacing, channel count and symbol rate. As a result, they offer a unique and comparable modem-independent measure of the optical performance of different subsea cables and designs.

The fundamental relationship for $OSNR_{ASE}$ and SNR_{ASE} has been defined in [27] in linear units as follows:

$$SNR_{ASE} = \frac{B_o}{\Delta f}\, OSNR_{ASE} \tag{5}$$

where,

B_o is the optical noise bandwidth in GHz used to define $OSNR_{ASE}$ (typically 12.5 GHz at 1550 nm)

Δf is the carrier spacing in GHz used to define $OSNR_{ASE}$ for a fully loaded system.

The underlying assumptions for the accuracy of this scaling is that the PSD is uniform within the bandwidth. This is only true in an ideal case where signals present a rectangular spectrum shape (root raised cosine with zero roll-off) and are spaced by their symbol rate. In such a case, the signal equivalent bandwidth B_e would numerically coincide with Δf.

When we consider a system operating with channel spacing Δf, and we deploy modems with $B_e < \Delta f$, those devices will experience a larger SNR_{ASE}. Even though $B_e < \Delta f$, most modern submarine modems achieve a bandwidth occupancy $\chi = B_e/\Delta f$ greater than 90% limiting the maximum SNR_{ASE} gap to <0.5 dB with respect to an ideal case with $\chi = 1$.

A similar scaling can be applied to the $GSNR$,

$$GSNR = \frac{B_o}{\chi \Delta f}\, GOSNR \tag{6}$$

Unlike the SNR_{ASE}, where only the total channel power matters, the bandwidth occupancy χ is now included as it has an impact of the $GOSNR$ calculation. The scaling of $GSNR$ among different channel plans depends on more factors and it is, in general, not straightforward. The channel bandwidth, shape and spacing as well as the dummy lights arrangement contribute to the SPM and XPM nonlinear noises.

It is beyond the scope of this work to analyze in detail such dependencies that can be explored by inspecting the GN formulation [1], [2], [28]. However, an illustrative example can be found in Fig. 2 for 100 repeater system in the C-band, with a 4.5 THz bandwidth, 90 km span length, and 150 μm^2 fiber effective area. The $GSNR$ penalty with respect to the ideal case ($\chi = 1$) is shown for different repeater TOP values. In the absence of fiber nonlinearity (dotted line), the reduction of bandwidth occupancy results in a $GSNR$ increase proportional to the reduction of the ASE noise bandwidth. In the presence of nonlinearity, the nonlinear noise grows stronger at lower χ due to SPM effects induced by the larger peak power of the channels.

As a general rule, we aim at keeping a large bandwidth occupancy, greater than 90%, to ensure a good matching between measurement scenario and the typical real use cases. In this regime, the $GSNR$ penalty is within +/− 0.5 dB for typical repeater TOP values. It is worth reiterating that the GSNR metric is independent of the modulation format. It is a wet plant parameter that depends on the line design and the input spectrum, mainly characterized by carrier spacing and symbol rate. Thus, the GSNR penalty shown in Fig. 2 shall be understood as the difference with respect to the maximum spectrum occupancy

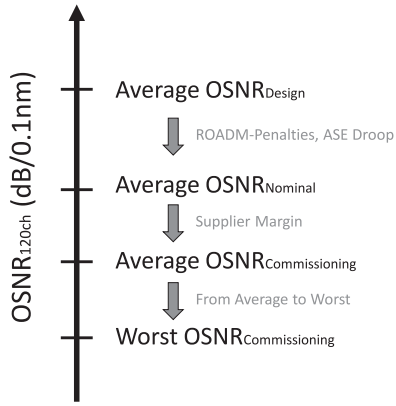

Fig. 1. OSNR Definitions for Subsea Open Cables.

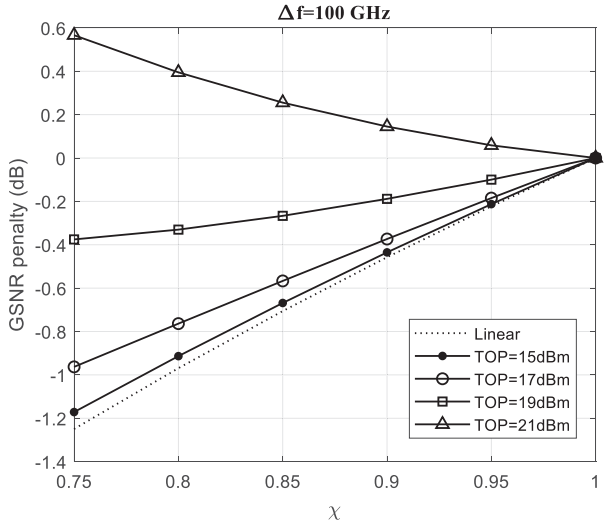

Fig. 2. Example of $GSNR$ penalty from the ideal $\chi = 1$ as a function of spectrum occupancy for different TOP values.

($\chi = 1$), which is an adequate baseline considering that it is the scenario where the GN model has analytical solutions. This GSNR penalty shall not be understood in data-rate or spectral efficiency terms.

C. GAWBS as a Noise Source

Guided Acoustic Wave Brillouin Scattering (GAWBS) is a spontaneous scattering of light in an optical fiber due to the interaction of transverse vibrational acoustic modes with light [20]. The spectrum of acoustic modes responsible for the light scattering in the forward direction oscillate at frequencies in the range of approximately 10 to 1000 MHz. Such modes modulate the refractive index of the fiber, inducing phase modulation on the propagating field which in turn can be converted both in amplitude and phase modulation of the signal at the receiver due to dispersion. The associated penalty of the effect to the transmission performance became measurable due to the introduction of low loss fibers in the dispersion uncompensated links and overall high signal to noise ratios required for transmission of high bit rate coherent signals [21]–[24].

It is important to properly account for the $GSNR$ penalty originating from GAWBS. In the experimental evaluation of GAWBS strength in the large effective area fiber $A_{eff} =$ 150 μm^2 GAWBS scattering coefficient, Γ_{GAWBS}, was found to be approximately -31 to -31.9 dB/Mm [21]. The strength of the scattering in single-mode fiber (SMF) was also experientially evaluated in [22]. Detailed theoretical calculation presented in [23] provided a close but somewhat larger value, $\Gamma_{GAWBS} = -30.2$ dB/Mm than in [21] for fiber with $A_{eff} = 150$ μm^2. Taking into account the experimental accuracy [21], [22] of directly measuring the strength of GAWBS it would be advisable to use theoretical number $\Gamma_{GAWBS} = -30.2$ dB/Mm for fibers with $A_{eff} = 150$ μm^2 as a more precise reference. It should be noted as well that for the smaller effective area fibers the strength of GAWBS is larger [21], [23]. GAWBS strength is estimated as $\Gamma_{GAWBS} = -29.6,\ -28.6,\ -27.5$ dB/Mm for the fibers with $A_{eff} = 130, 110, 80$ μm^{2}correspondingly based on the relative dependencies on the effective areas provided in [21], [23]

The related question is what impact GAWBS has on the performance of a coherent receiver; one might note [22], [24] that since GAWBS creates phase distortions/modulation at point of origin it can be potentially compensated by DSP, for example by fast adaptive linear equalizers and phase tracing algorithms.

The compensation methods considered in [22] are complex and demonstrated only for short distances. It was shown in [24] that compensation will be difficult due to the linewidth about 10 MHz of individual acoustic modes contributing to the signal scattering. It means that DSP algorithms need to be capable of tracking distortions with the frequencies exceeding 10 MHz which is difficult to achieve. Thus, for practical purposes GAWBS contribution will be treated as an extra noise source affecting coherent receiver performance.

GAWBS is a narrowband effect which scatters light within channel bandwidth itself. This means that in the process of typical OSNR system characterization it will not be measured directly and accounted for. The most convenient option for evaluating GAWBS SNR penalty is analytical estimation: one can calculate GAWBS GSNR contribution in linear units after transmission distance *L*:

$$SNR_{GAWBS} = \frac{1}{\Gamma_{GAWBS} * L} \tag{7}$$

And total $GSNR$ of the system can be calculated as:

$$\frac{1}{GSNR} = \frac{1}{SNR_{ASE}} + \frac{1}{SNR_{NLI}} + \frac{1}{SNR_{GAWBS}} \tag{8}$$

D. Inclusion of Signal Droop

SDM cables have enabled more capacity by multiplying the number of fiber pairs in the cable at the expense of channel SNR_{ASE}. Consequently, in low SNR_{ASE} environments the noise accumulation under fixed total output power constraints depletes signal power. This depletion of signal power (or droop) can be formulated through the product rule for inverse droop [25]:

$$1 + \frac{1}{SNR_{1\to N}} = \prod_{k=1}^{N}\left(1 + \frac{1}{SNR_k}\right) \tag{9}$$

where N represents the amplified span, and SNR_k the SNR_{ASE} at the output of the k^{th} amplifier. This SNR degradation law can be extended to all AWGN sources within the signal bandwidth, for example GAWBS, nonlinear noise, ASE, crosstalk, etc. Thus, the inverse droop formula is re-arranged into a Generalized Droop formula to account for the aggregation of multiple Gaussian noise sources [29]:

$$1 + \frac{1}{GSNR} = \left(1 + \frac{1}{SNR_{ASE}}\right)\left(1 + \frac{1}{SNR_{NLI}}\right) \times \left(1 + \frac{1}{SNR_{GAWBS}}\right) \tag{10}$$

III. Measurement of GSNR

Considering the newly expanded definitions discussed thus far, this section will expand upon previously proposed measurement methodologies in [12], for $GSNR$ and SNR_{TOT}. Here, we discuss the physical demarcation definitions, expand the methodologies for wet plant measurement to enable alignment with evolving modem technology trends, and discuss the impact of the modem as a measurement tool.

A. Open Cable Interface as a Demarcation Point

Before discussing the measurement procedures of *GSNR*, it is important to note that the performance impact of the equipment appended to the subsea cable, either permanently, or for the purposes of measurement, must be considered. It is entirely up to the purchaser and supplier to determine whether the SNR_{ASE} and $GSNR$ specifications for a subsea cable will include this added optical equipment or not, what is important is that this is clearly defined.

It is common for subsea cables to be bookended at their termination points by an Open Cable Interface (OCI). The OCI encompasses all optical equipment provided by the system supplier that remains permanently within the optical propagation path after system handoff. The OCI should also

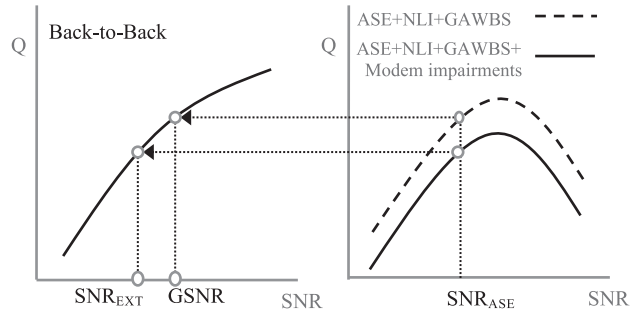

Fig. 3. ***GSNR*** measurement concept using a coherent modem. Solid lines are measured performance, back-to-back and after transmission. The dashed line illustrates the effect of modem impairments.

provide the ability to couple the wet plant supervisory and monitoring equipment, without dependency on the selection of terminal transmission equipment (TTE), which may be provided by a 3rd party as part of the Open Cable concept.

The OCI provides a clear demarcation for the handoff between the subsea system and the TTE that will be overlaid onto it. The handoff between these two sets of equipment should be clearly defined, with minimum and maximum optical input and output power targets, to minimize unnecessary optical performance penalties.

It is recommended here that this demarcation point should also define the point at which SNR_{ASE} and $GSNR$ are measured at cable acceptance. Any additional contributions from the TTE optical components can be considered independently of the cable build, and no joint analysis required by wet plant and TTE equipment vendors.

B. GSNR Measurement: Inverse Back-to-Back Method

In this section, a method is introduced to measure the $GSNR$ of a transmission line. This procedure is based on two fundamental ideas or conditions:

1) The transmission line can be well modeled by the GN model [1], [2]
2) Digital coherent modems show a predictable dependency of BER with fiber nonlinear effects and GAWBS.

If these two conditions are met, the inverse back-to-back method [8] can be used to estimate the $GSNR$ of a transmission line. The inverse back-to-back method translates a Q-value into an equivalent SNR value. This method is accurate in systems where nonlinearity and GAWBS induce Gaussian-like noise, which enables the use of the back-to-back curve for Q-to-SNR conversion. First, a pair of test modems are characterized by measuring the Q-value in a back-to-back configuration, with ASE loading. This process generates the so-called, SNR_{ASE}-sensitivity curve (or *back-to-back* curve), where the Q-value is obtained as a function of SNR_{ASE} without any transmission impairments. Then, the same modem pair is connected to the submarine line, and the Q-value is obtained, now including all transmission impairments. This Q-value is mapped into the back-to-back curve to obtain a resulting SNR value, SNR_{EXT}. This method is schematically shown in Fig. 3. After transmission, the Q-value includes penalties coming from the transmission line (such as fiber nonlinearity or GAWBS) and transmission penalties induced by the modem.

Now, the measured SNR_{EXT} has been obtained via the inverse back-to-back method, i.e., $SNR_{EXT} = \mathrm{iBtoB}(Q)$, where iBtoB is the function that converts Q into SNR from the back-to-back performance, as previously discussed. Then, the contribution of the modem impairments is subtracted to finally obtain the GSNR:

$$\frac{1}{GSNR} = \frac{1}{SNR_{EXT}} - \frac{1}{SNR_i} \tag{11}$$

SNR_i includes the noise caused by the modem due to propagation specific effects such as chromatic dispersion, polarization effects, wavelength tolerance penalties and equalization enhanced phase noise.

Polarization effects such as polarization dependent loss (PDL), polarization mode dispersion (PMD) or polarization transients are unique to each cable system and can be partially compensated by the coherent receiver. Due to the statistical nature of these effects, care should be taken to consider the mean of the polarization impairments from both the cable system and the coherent receiver [30].

The applications of digital chromatic pre- or post-dispersion compensation are implemented by DSP filters. The implementation penalty of these filters should be considered as they may not be present in back-to-back measurements. Ideally chromatic dispersion should be either compensated in the transmitter or receiver since balanced compensation provides a nonlinear benefit, thereby artificially improving the cable system's $GSNR$.

Wavelength tolerance impairments correspond to degradations due to non-optimal wavelength settings [31]. These can range from crosstalk penalties to ROADM filter penalties on a channel.

The interaction between the chromatic dispersion compensation filter (or 'equalizer') and the phase noise of the local oscillator (LO) laser in the coherent receiver generates an impairment called equalization enhanced phase noise [32]. This penalty increases with high dispersion systems where the frequency noise of the LO is enhanced by the electronic equalization.

The impairments considered above may not be an in-situ measurement with the cable system under test. These are primarily simulated and aligned with controlled lab measurements. The magnitude of these penalties can influence an undersea system's $GSNR$ depending on the coherent technology and performance budget set for them.

The first step to measure the $GSNR$ is, therefore, to obtain the conversion function. SNR_{ASE} has been traditionally used to characterize the performance of modems. Typically, a test modem is connected back-to-back (i.e., TX-to-RX) with a Gaussian noise source in between and adjacent channels loaded next to the test modem to account for WDM filtering penalties or inter-channel crosstalk. This is shown in Fig. 4.

Recently, some alternate methods have been proposed to estimate the ASE and NLI contributions to the SNR. One technique is based on the evaluation of the spectral broadening of a channel after transmission but using an Optical Spectrum Analyzer [33].

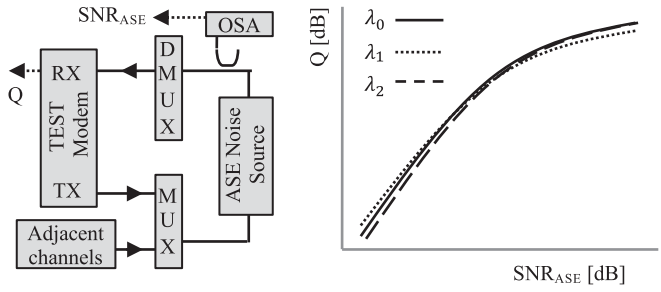

Fig. 4. Diagram of the $\boldsymbol{SNR_{ASE}}$ sensitivity of a modem.

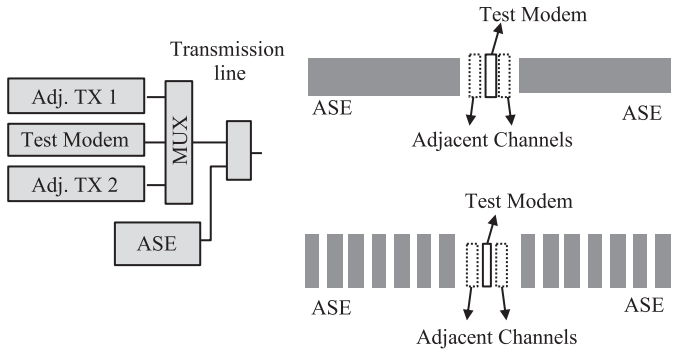

Fig. 5. Configuration of the $\boldsymbol{GSNR}$ measurement at the transmitter with continuous or channelized dummy lights.

Another technique consisted in measuring some noise correlations within the channel bandwidth by using a broadband ASE as light source [34]. Similarly, the noise correlations of received symbols of a coherent modem, together with neural networks techniques, have been proposed to separate the ASE and nonlinearity noise contributions retrieved from the received symbols [35].

It is not yet clear whether proposed methods can achieve sufficient accuracy or universality. Although they can be useful in some applications, (for example in service $GSNR$ estimation), we believe that the inverse back-to-back method with well-known test modems is the preferred method for the evaluation, commissioning and capacity estimation of open cables.

C. Measurement Conditions: Input and Output Spectra

One of the targets of $GSNR$ measurement is to enable estimates of the total achievable capacity that can be supported by the transmission line. For that, measurements must be conducted across the usable bandwidth. In general, due to the frequency dependency of amplifier noise figure, scattering effects, gain shape and tilt, among others, optical signals experience frequency-dependent power and SNR variations as they propagate along the fiber. This relationship with frequency also varies notably with different input power profiles, due to the power limited nature of the subsea repeater, and the frequency-dependent nature of spectral hole burning (SHB). Thus, SNR_{ASE} and $GSNR$ will always vary across an optical spectrum and as a consequence of the aforementioned dependencies, the input power profile must be very carefully taken into account in any SNR_{ASE} or $GSNR$ measurement.

It is generally agreed today that populating the entire spectrum with test modems to conduct the $GSNR$ measurement is impractical. It is proposed to use a minimum of 3 channels and ASE as dummy lights for the remainder of the optical spectrum. The frequency of the test modem and the adjacent channels can be tuned to cover the entire transmission waveband. The ASE dummy lights could be continuous or channelized. The advantage of channelized dummy lights is that they can also be used to measure the SNR_{ASE}.

The test modem and the adjacent channels are tuned across the usable bandwidth to sample and obtain a view of the frequency dependency of the $GSNR$. Fig. 5 shows the measurement configuration for $GSNR$ measurement.

Three typical configurations may be of interest for $GSNR$ measurements, namely: Flat transmitter power (FLAT), SNR_{ASE}-equalized power (SNREQ), and fiber-power equalized (PFIB). These configurations are schematically shown in Fig. 6. These configurations are achieved by adjusting the channel pre-emphasis of the channels. For example, for Flat transmitter power, the channel pre-emphasis is set to equalize the power spectral density at the transmitter (i.e., same density for dummy light and test channels). In other cases, the pre-emphasis value is adjusted depending on the received power or SNR_{ASE}.

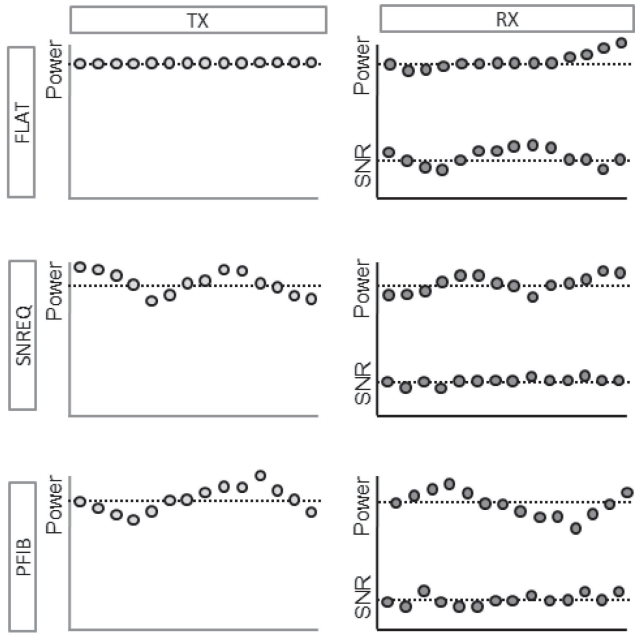

Fig. 6. Pre-emphasis settings for $GSNR$ measurement. Arbitrary shapes are shown for explanation purposes.

In the case of FLAT equalization input spectrum is flat, where the power is equal at every wavelength. In the case of SNREQ power of each wavelength at the transmitter is adjusted to achieve a uniform SNR_{ASE} across the received bandwidth. Finally, the PFIB equalization consists in equalizing the sum of transmitter and receiver power. FLAT equalization is useful to determine the gain and tilt characteristics of the line and would theoretically be the optimum in the absence of any of the frequency dependencies noted previously. SNREQ equalizes the linear part of the $GSNR$ whereas PFIB attempts to take into account the nonlinear contribution as well as the linear contribution to $GSNR$.

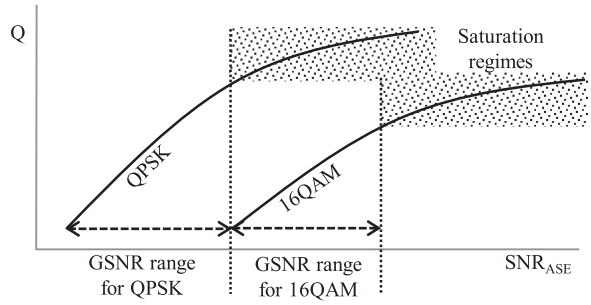

Fig. 7. Expansion of the $GSNR$ measurement range by using multiple modulation formats operating at the non-saturated regime.

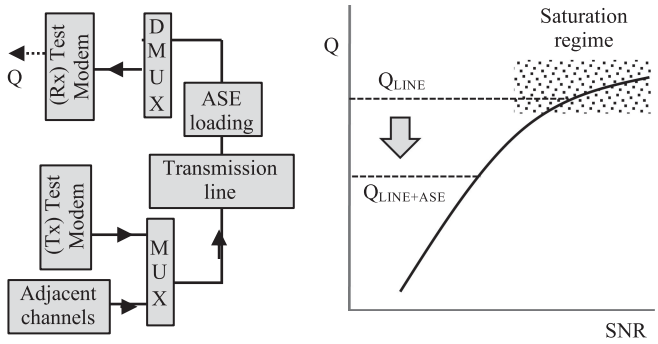

Fig. 8. Expansion of the $GSNR$ measurement range by using ASE loading at the receiver.

It is worth noting that we are not attempting to equalize the $GSNR$, as such equalization may not result in the maximum fiber capacity if, for example, NLC techniques are implemented in the modem. These three equalization profiles can be used to characterize the fiber transmission line, however, depending on the design and the $GSNR$ wavelength dependency, it may not be necessary to conduct the measurement in all the three configurations. A detailed discussion of pre-emphasis equalization strategies and system capacity is done in [36].

D. Characteristics of the Test Modem

The desired test modem for the $GSNR$ measurement must be able to provide stable and accurate results over a wide range of transmission lines. The following are some generally agreed recommendations for standard specifications of a $GSNR$ test modem:

1) *Modulation format:* dual polarization QPSK and dual polarization 16QAM
2) *Carrier spacing for adjacent channels:* ∼1.1 x symbol rate
3) S*pectral shaping:* RRC with ∼0.1 roll-off
4) *Chromatic Dispersion Compensation:* CDC range compatible with the transmission line
5) *Nonlinearity compensation:* Disabled
6) *DSP:* Typical methods for carrier phase recovery, polarization DEMUX and cycle slip protection.

It is desired that the test modem operates at a symbol rate that provides an SNR_{ASE} sensitivity curve with sufficiently large slope, avoiding the saturating regime of the Q-vs-SNR performance. This could be a problem to be outside the range of a particular modulation format. This is illustrated in Fig. 7, where the test modem shall be capable of operating at QPSK and 16QAM in order to cover a wide range of SNR_{ASE} values without entering the more unstable saturation regimes.

The saturation characteristics depend on the modem implementation, but typical coherent QPSK modems can be used for a wide range of $GSNR$ values. However, in very high $GSNR$ environments where QPSK is limited to the saturation regime, 16QAM is used as an alternative.

Another potential solution to avoid the saturation regime of the back-to-back curve is to load ASE noise at the receiver. This is shown in Fig. 8 , where a source of ASE is located between the transmission line and the receiver to shift the Q value away from the saturation regime.

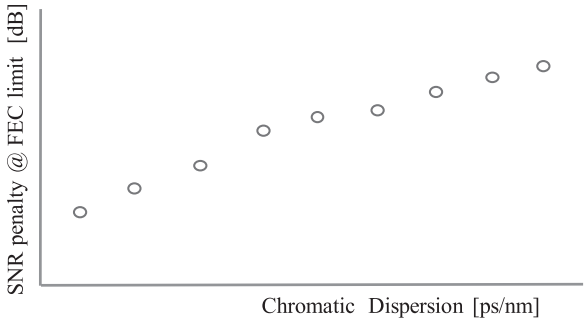

Fig. 9. SNR penalty caused by the compensation of chromatic dispersion in the modem DSP.

E. Estimation of Modem Impairments

It is important to understand and separate modem-dependent contributions to the *GSNR*, especially in wet plant commissioning applications. In this section, we introduce some example approaches that can be taken to separate these contributions, however different modem vendors may employ different methodologies best suited to their particular technology. Perhaps the most straightforward example is the CDC penalty, which greatly depends on the effective filter size implemented in the modem DSP. In order to understand and separate this contribution, it is important to characterize the performance of the test modem as a function of the chromatic dispersion. For that, it is convenient to obtain the SNR penalty caused by chromatic dispersion. This penalty can be relative to the SNR_{ASE} value of the test modem at the FEC limit, which is a typical procedure to determine performance penalties. Then, it can be converted to RX noise and subsequently subtracted to the $GSNR$ measurement as a contribution of SNR_i.

Another approach to estimate the modem transmission penalties is experimentally isolating the contribution of fiber nonlinearity [10]. For that, the Q-performance can be obtained as a function of the channel pre-emphasis under propagated conditions. This Q-variation is only caused by fiber Kerr effect, and it can be modelled and estimated by the GN model with the transmitted spectrum as the input. By comparing the experimental values with the model, the contributions of fiber nonlinearity and modem penalties can be separated using a minimum-square fitting. For that, let us define the following transmission-impairment magnitude (experimentally obtained),

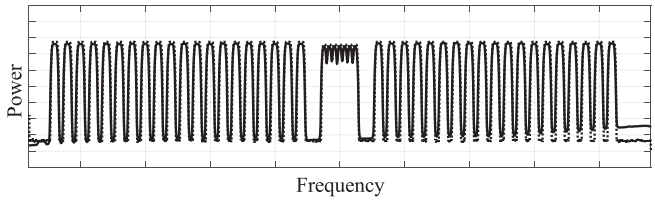

Fig. 10. Example of the WDM configuration to calculate G_{wdm} as a function of the channel pre-emphasis (PE). Solid line is the experimental spectrum, and dashed line is the mathematical representation used in (14).

SNR_{TI_E}, as a function of the channel pre-emphasis (PE):

$$\frac{1}{SNR_{TI\_E}(PE)} = \frac{1}{SNR_{EXT}(PE)} - \frac{1}{SNR_{ASE}(PE)} \tag{12}$$

where SNR_{EXT} and SNR_{ASE} are the parameters defined previously and they are both measured experimentally. Alternatively, the same magnitude can be defined theoretically, SNR_{TI_T}, from the following expression:

$$\frac{1}{SNR_{TI\_T}(PE)} = \frac{1}{SNR_{NLI\_GN}(PE)} + \frac{1}{SNR_{GAWBS}} + \frac{1}{SNR_i} \tag{13}$$

SNR_{NLI_GN} can be obtained from the GN model equations by using, as inputs, the transmitted spectrum (or a close mathematical representation) and the nominal measured data of the as-laid wet plant, such as number of spans, repeater total output power, fiber attenuation, span loss, effective area, and fiber dispersion. The magnitude, SNR_{GAWBS} is known and calculated from (7). Note that the contribution SNR_i is assumed to be independent of the power pre-emphasis, accounting for transmission impairments such as CD, PMD and PDL penalties.

In practice, it is difficult to vary the repeater output power and therefore it is common practice to vary the power of only a few channels with the channel under test at the center of them. Since this calculation needs to model the pre-emphasis of only a few channels while keeping the total power constant, the full integration of the GN is required for the channel under test, as follows:

$$SNR_{NLI\_GN} \propto \iint_{-\infty}^{+\infty} G_{wdm}(f_1, PE) \times G_{wdm}(f_2, PE) \times G_{wdm}(f_1 + f_2 - 0, PE) \times \rho \times \chi \, df_1 df_2 \tag{14}$$

Where PE denotes the pre-emphasis of the measured channel. More details of this and the parameters therein can be found in [28]. The spectral density function G_{wdm} is defined to match the experimental conditions of the measurement. An example is shown in the Fig. 10.

Once the theoretical value, SNR_{NLI_GN} is obtained, both expressions, SNR_{TI_E} and SNR_{TI_T} are compared and the value of SNR_i is obtained to best fit both curves as a function of the channel pre-emphasis. Fig. 11 shows an example of this fitting obtained experimentally in an approximately 7,000 km straight-line transmission test with a 34 Gbaud QSPK transponder. The agreement is good for a wide range of channel pre-emphasis. This technique relies on the accurate representation of the as-laid wet plant by the GN model, this can be verified by the fitting error as a function of the deviation from the nominal wet plant parameters that can be directly measured.

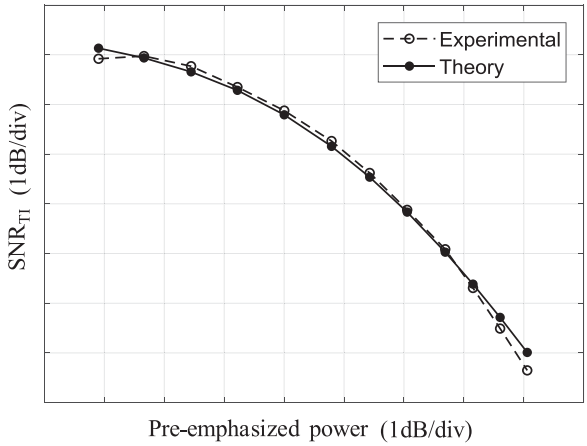

Fig. 11. Example of the fitting between SNR_{TI_E} and SNR_{TI_T} after Minimum Square fitting with the single parameter optimization of SNR_i

F. Avoiding SHB During the Measurement Procedure

As we saw previously, different SNR_{ASE} values can be defined as Design, Nominal, or Commissioning, not all of which can be measured. The accuracy that should be reached in the measurement of SNR_{ASE} should be of the utmost importance for a number of reasons. First, the acceptance of the submarine cable is linked in part to the measurement of this value which will in turn be compared to the values specified in the contract. Second, in D+ subsea designs, SNR_{ASE} is the largest relative SNR contribution to the end to end optical performance [37].

There are various methodologies employed for measurement of SNR_{ASE} in subsea systems. A key concern, in particular in the subsea environment with fixed TOP repeaters, is the impact of SHB. A method was presented in [11] allowing to limit the impact of SHB on the accuracy of the SNR_{ASE} measurements. In one classical method to measure SNR_{ASE}, the power of the channel is measured, and then with the channel removed, the power of the noise is measured. In an experiment presented in [11], doing this resulted in varying the number of channels from 56 to 55, corresponding to an average power variation below 0.1 dB. Nevertheless, this experiment showed that due to SHB, after 11,000 km, local variation differs by 0.5 dB in the measured noise floor. This error is not acceptable considering the supplier margin taken previously. To improve the accuracy of the measurement, the solution proposed in [11] was to replace the channel under test by a depolarized laser that will be set at the same power. This substitution was shown to allow an accurate representation of the channel's noise under full-fill conditions. This is illustrated in Fig. 12, where we can see three different spectra:

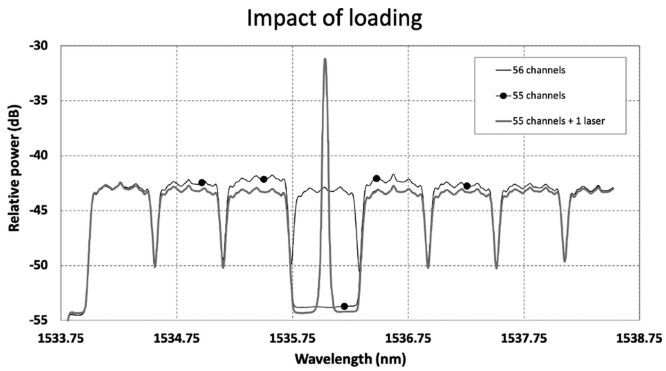

Fig. 12. Impact on the amplifier gain due to spectral hole burning over 11,000 km when a channel is removed and replaced by a laser source [11]

- the initial spectrum (black usually under the grey spectrum) around 1536 nm with 56 channels
- the intermediate spectrum (black with circle) with 55 channels where the channel under test is removed
- the final spectrum with 55 channels + 1 laser (grey) when the laser is added.

We can clearly see that after the laser has been added we are recovering back the initial spectrum (grey spectrum overlaps black spectrum).

IV. Capacity of Open Cables

In this section we change perspective shifting from defining and measuring key metrics representing the optical performance of the wet plant in isolation, to considering the noise contributions of the modem, and as such, the end to end system capacity. We describe the evolution of per fiber pair (FP) performance modeling and calculation to a whole cable approach. The fundamental paradigm shift brought by SDM in the submarine industry is especially valuable when we can consider the whole cable as an entity, instead of the individual FPs. With a whole cable approach, we can improve the total cable capacity at the expense of the individual FP capacity [19]. In the next paragraphs we will give the equations to operate on whole cable capacity and to cascade multiple segments (e.g. branches) of a cable system.

A. Evaluation of SNR_{TOT}

The total signal-to-noise ratio SNR_{TOT} affecting the signal at the decoder input, within the modem DSP, is a superposition of all noise terms: NLI, ASE, GAWBS, signal droop, and modem related contributions including relevant receiver scaling factors. Real-time SNR_{TOT} is a computed performance metric, using an empirical relationship between SNR_{TOT} and the Q-factor. Assuming Gray encoding and high SNR_{TOT} so that off-axis bit error probabilities are negligible [38]–[40], Table I provides examples of closed form solutions for this relationship. As noted in Section I, in this paper, we use Q to represent Q^2 factor.

Recent advancements in coherent optical technologies embrace higher constellation cardinality, stronger FEC engines that operate at very low SNR_{TOT}, and novel bit-to-symbol encoding formats [41], [42] which no longer hold a closed form analytical solution for Q as a function of SNR_{TOT}. Subsequently, the Q for each modulation format at a given SNR_{TOT} is achieved through widely used numerical techniques such as the Monte-Carlo method [43]. The technique passes many data symbols through a model of the modem and the SNR_{TOT} is varied by injecting additive white Gaussian noise along the data path. The symbols are decoded by the simulator and the bit errors counted to estimate the Q using the inverse complementary error function $Q = \sqrt{2}\mathrm{erfc}^{-1}(2\mathrm{BER})$, thus forming a relationship between SNR_{TOT} and Q.

TABLE I
Closed-form SNR and Q relationships

Modulation	Q
BPSK	$\mathrm{Q} = 2SNR_{TOT}$
QPSK	$\mathrm{Q} = SNR_{TOT}$
16PSK	$\mathrm{Q} = 2SNR_{TOT}\, sin^2\left(\frac{\pi}{16}\right)$
16QAM	$Q = \left(erfc^{-1}\left[\frac{3}{4}erfc\left(\sqrt{2SNR_{TOT}/5}\right)\right]\right)^2$

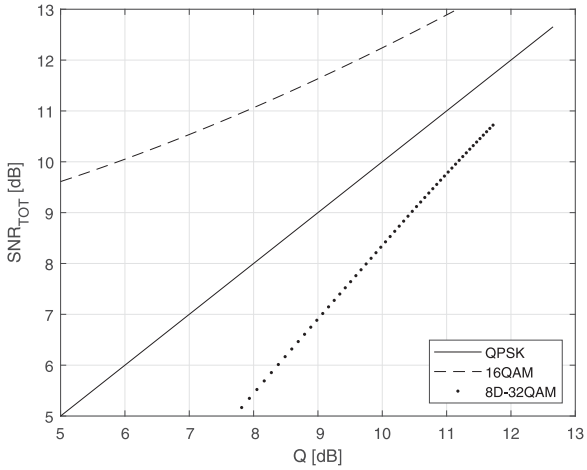

Fig. 13 Monte-Carlo calculation of the $\boldsymbol{SNR_{TOT}}$ to Q relationship

Fig. 13 shows an example of the relationship between Q and SNR_{TOT} for three different modulation formats; QPSK, 16-QAM, and a modern eight-dimensional 32-QAM format. The QPSK and 16QAM curves follow the relationships in Table I, however modern formats may require a piecewise curve fit.

In the presence of optical noise loading, the ASE noise is varied which in turn varies the Q-factor reported by the modem. For a back-to-back configuration, the total SNR is directly proportional to $1/SNR_{ASE}$:

$$\frac{1}{\mathrm{SNR}_{\mathrm{TOT}}^{b2b}} = \frac{1}{\mathrm{SNR}_{\mathrm{ASE}}^{b2b}} + \frac{1}{\mathrm{SNR}_{\mathrm{m}}} \tag{15}$$

$$\frac{1}{SNR_{TOT}} = \frac{1}{\dfrac{1}{\dfrac{1}{SNR_{ASE}} + \dfrac{1}{SNR_{NLI}} + \dfrac{1}{SNR_{GAWBS}}}} + \frac{1}{SNR_i} + \frac{1}{SNR_m}$$

Fig. 14. Full description of SNR_{TOT}

Where, SNR_m is a back-to-back implementation noise due to the coherent modem. Under propagation the total SNR of the optical link is described by:

$$\frac{1}{SNR_{TOT}} = \frac{1}{\mathrm{GSNR}} + \frac{1}{\mathrm{SNR_m}} + \frac{1}{\mathrm{SNR_i}} \tag{16}$$

It is important to discuss the relationship between SNR_{TOT} and SNR_{EXT}, as defined in the previous section. Due to the nature of the inverse back-to-back method described in Section III-B, the SNR_m contribution is directly removed, leaving the following relationship:

$$\frac{1}{SNR_{EXT}} = \frac{1}{SNR_{TOT}} - \frac{1}{SNR_m} \tag{17}$$

Now that all SNRs have been defined, we can summarize the complete relationship with SNR_{TOT} as shown in Fig. 14.

B. From GSNR and SNR_{TOT} to Cable Capacity

Shannon's equation for capacity in AWGN channel would apply perfectly to our case in the absence of nonlinearities, i.e., with ASE as the only noise source. In such a case we could write:

$$C = 2B\log_2\left(1 + SNR_{ASE}\right) \tag{18}$$

where B is the optical bandwidth over which we have a signal-to-noise ratio of SNR. The factor of 2 comes from the degenerate spatial dimension in the optical channels: the orthogonal polarizations.

In a submarine cable having N_{FP} fiber pairs we could measure the $GSNR_i(f)$ on the i^{th} FP, as a function of the optical frequency f. In that case, the total theoretical cable capacity C can be calculated as:

$$C = 2\sum_{i}^{N_{FP}} \int_{-B_i/2}^{+B_i/2} \log_2\left[1 + GSNR_i\left(f\right)\right] df \tag{19}$$

where B_i is the size of the bandwidth on which the $GSNR$ is calculated. This equation implies that now linear and nonlinear effects, under the GN model, with the addition of GAWBS can be used to determine the theoretical capacity of the submarine system. Future modem implementations designed with strong nonlinear compensation capabilities might even exceed this capacity, which is not an upper bound like (18). In the case where B_i are all identical across all FPs and small enough so that $GSNR_i(f)$ is constant in the j^{th} frequency bin, then we could consider a simplified version of (19) which calculates capacity as:

$$C = 2B\sum_{i}^{N_{FP}} \sum_{j} \log_2\left(1 + GSNR_{i,j}\right) \tag{20}$$

where B is the total repeater bandwidth. So far, the cable capacity returned by the equations is a theoretical cable capacity. In a more practical case, we might want to know the actual capacity that we could get with a specific modem. For instance, a previously characterized modem, not necessarily the same used for the $GSNR$ measurement of the wetplant. We assume that the modem is modeled knowing the parameters from (16) which allows us to express the capacity in terms of $\mathrm{SNR_{TOT}}$:

$$C_{modem} = 2\chi B\sum_{i}^{N_{FP}} \sum_{j} \log_2\left(1 + \frac{SNR_{TOT\ i,j}}{\eta M}\right) \tag{21}$$

where η is a gap-to-Shannon value expressing the non-ideal characteristic of a linecard (e.g. finite length FEC limiting its performance) to be characterized for every modem, M is a system margin that the cable operator might find appropriate and χ accounts for the spectral occupancy with a given modem.

In this context one can appreciate the great value of $GSNR$ as a universal metric. In the previous sections we discussed how to measure the $GSNR$ of a FP with any modem; in this second step we discover that from such a $GSNR$ we can determine the potential capacity with any other kind of modem (e.g. we are considering an upgrade for our cable system) under the same power pre-emphasis conditions. Of course, this equation is convenient for system design because it presents a continuous behavior, but it still misses one important aspect of modems, the line rate quantization. Even though such quantization proved to be an important aspect in the selection of a modem [36], we consider that those considerations are beyond the scope of this paper.

C. Multi-Segment Considerations

There are some instances in which an all-optical interconnection of multiple segments may be desired. In this section, we discuss a method for assessing this kind of interconnection, noting that it can only be used where the characteristics of each segment are such that they ensure the validity of the GN model.

As outlined in II-A the formula for determining the Design OSNR assumes the same average gain and noise figure for amplifiers in a system with a constant amplifier output power. In multi-segment systems the assumptions of the system having constant TOP, amplifier spacing and fiber composition across all segments typically cannot always be made. As a result, in multi-segment systems the SNR for each segment, SNR_k, must be determined for the same channel loading and added together to calculate the end to end SNR, SNR_{E2E}.

$$\frac{1}{SNR_{E2E}} = \sum_{k}^{N_{segments}} \frac{1}{SNR_k} \tag{22}$$

$GSNR$ can be measured across the multi-segment system or, much like SNR, $GSNR$ of each segment can be concatenated to calculate the $GSNR$ of an end to end system.

$$\frac{1}{GSNR_{E2E}} = \sum_{k}^{N_{segments}} \frac{1}{GSNR_k} \tag{23}$$

For $GSNR$ values to be valid the system must have enough dispersion in each segment to ensure the GN model applies. Short network segments or terrestrial segments with non-D+ fiber (e.g. LEAF, DSF, etc.) may not have enough dispersion for the GN model to apply.

In networks such as this an end to end measurement of $GSNR$ may not align to the expected values from mathematical concatenation of per segment $GSNR$.

V. Open Cable Specification Tables

Implementation of the Open Cable concept for cable design, acceptance and TTE deployment requires clear specification of key system parameters and performance metrics at all stages of a subsea cable project. These specifications should allow for capacity estimation prior to TTE deployment, both during the design phase and following cable commissioning and acceptance with the highest degrees of accuracy possible at the time. To address this goal, we discuss recommended tables to describe and record key parameters of the wet plant and introduce SNR-based optical performance budget tables for the key disaggregated elements of an Open Cable system: the wet plant and the TTE.

A. Key Parameter Table

The Key Parameter Table (KPT) is a table which contains important metrics and parameters that define the optical performance and the underlying system characteristics that contribute to it, allowing for the computation of nominal performance metrics. These parameters are essential to an Open Cable purchaser in understanding the asset they are purchasing. This table also serves the critical function of capturing some of the fundamental optical specifications required for end to end capacity estimation by a TTE vendor, using their specific modem technology, in advance of the completion of the system. The KPT is most commonly used during the design phase of an Open Cable project, however it is customary for this table to be updated over the course of the project construction to reflect any system design changes that occur, such as additional repeaters. A recommendation for a KPT is presented in [12].

Many of the parameters within the KPT are defined as average values, without specific reference to frequency, temperature, or manufacturing variations. Some values can be an average with respect to a system component as determined from manufacturing distributions, as well as an average with respect to frequency, such as repeater noise figure. It is not until system completion that detailed measurements are made to capture the frequency and pre-emphasis dependencies of the key performance metrics, such as SNR_{ASE} and $GSNR$. It is important for such detailed frequency-dependent data to be collected, even though it is customary that only the average values of a few key parameters are compared against agreed minimum performance targets, or the commissioning targets, and used for commercial acceptance of the system. These detailed measurements, reported with respect to specific test conditions, are highly critical to accurate capacity modeling of a given optical path within an Open Cable system and can only be collected once the system is constructed. An example table to guide the capture of critical system data to be collected is provided in [12].

While the KPT has traditionally contained the final agreed commissioning values, it does not detail the various SNR contributions and margins used to reach these performance targets. The SNR-based optical performance budgets in the following sections are provided to capture these details.

B. SNR Budget Table for Wet Plant

The proposed SNR Budget Table summarizes the various noise sources that contribute to the final SNR-based commissioning targets of the Open Cable. It is typical that the Beginning-Of-Life (BOL) Average and Worst Case SNR targets for SNR_{ASE} and $GSNR$ are agreed as commissioning targets under specific pre-emphasis conditions. These values have traditionally been defined in the corresponding KPT, and demonstrated during cable commissioning. With the introduction of Table II, we propose that the agreed commissioning parameters no longer need to be specified in a KPT, as they can be agreed and more clearly represented within Table II. Only select line items in Table II are measurable quantities, and as such many of the SNR values listed are treated as informational and are primarily requested for the purposes of design evaluation. The table displays both absolute SNR quantities as well as the dB difference between line items as an ‘SNR Change’. Example values for a representative modern subsea open cable are provided to illustrate both the application of the proposed tables and approximate order of magnitude that may be expected. While both SNR and SNR Change can be provided for each line, only the form for which a given line is most commonly discussed is listed for simplicity. All values listed will vary according to the particular system design and vendor specifics.

TABLE II
WET PLANT SNR BUDGET TABLE

	Segment Information	SNR [dB]	SNR Change [dB]
	SNR_{ASE}		
1.0	Design	13.2	
1.1	Signal Droop		0.2
1.2	Wet Plant ROADM		0.1
1.3	Terrestrial Extension		N/A
1.4	Nominal	12.9	
1.5	Supplier Margin		0.2
1.6	BOL Average Flat Launch	12.7	
1.7	Pre-Emphasis Margin		0.4
1.8	BOL Average (EQ)	12.3	
1.9	BOL Worst Case (EQ)	11.4	
1.10	Aging and repairs		1.4
1.11	EOL Average (EQ)	10.9	
1.12	EOL Worst Case (EQ)	10.0	
	GSNR		
2.0	GAWBS	25.9	
2.1	Optical Nonlinearity	15.7	
2.2	Nominal	11.1	
2.3	Supplier Margin		0.3
2.4	BOL Average Flat Launch	10.8	
2.5	Pre-Emphasis Margin		0.3
2.6	BOL Average (EQ)	10.5	
2.7	BOL Worst Case (EQ)	9.0	
2.8	EOL Average (EQ)	9.3	
2.9	EOL Worst Case (EQ)	8.7	

Line 1.0: The design SNR_{ASE} of the submarine portion, averaged across the band.

Line 1.1: Signal droop impairments in SNR_{ASE} due to noise accumulation from ASE.

Line 1.2: The SNR_{ASE} impairment from any ROADMs in the submarine portion.

Line 1.3: Impairments arising from the terrestrial extensions and/or any unrepeatered branch, if applicable.

Line 1.4: The nominal SNR_{ASE} on Line 1.4 for the system is the subtraction of Lines 1.1, 1.2 and 1.3 from Line 1.0.

Line 1.5: The supplier margin provides allocation for normal product variations due to the manufacturing process, marine operations and environmental conditions.

Line 1.6: This is the system average SNR_{ASE} under flat launch conditions at BOL. Line 1.6 SNR_{ASE} is given by subtracting Line 1.5 from Line 1.4.

Line 1.7: Represents the penalty experienced by the average SNR_{ASE} due to pre-emphasis based equalization under non-flat gain conditions, relative to the average SNR_{ASE} under flat launch conditions. This form of equalization is typically performed with the intent of improving the performance of the worst case channel(s). There are various methods of equalization which can be selected from with comparable merits [36].

Line 1.8: Represents the average SNR_{ASE} after equalization has been applied. Line 1.8 SNR_{ASE} is calculated by subtracting Line 1.7 from Line 1.6. This represents the commissioning limit for the average equalized performance at BOL.

Line 1.9: This is the allowance for spectral variation of performance across the band. The values correspond to the worst case SNR_{ASE} across the band after equalization. This value may be agreed as a commissioning target.

Line 1.10: Represents the SNR_{ASE} penalty due to repairs and aging of the interoperable cable portion.

Line 1.11: Represents the average SNR_{ASE} after equalization has been applied under End-Of-Life (EOL) conditions. Line 1.11 SNR_{ASE} is calculated by subtracting Line 1.10 from Line 1.8.

Line 1.12: This is the allowance for spectral variation of performance across the band. The values correspond to the worst case SNR_{ASE} across the band after equalization under EOL conditions.

Line 2.0: The SNR impairment due to GAWBS.

Line 2.1: The noise contribution of optical nonlinearities or SNR_{NLI}.

Line 2.2: The nominal $GSNR$ is calculated using the generalized droop formula, as defined in Section II-D. The SNR_{ASE} is referenced at Line 1.4, SNR_{GAWBS} from Line 2.0, and SNR_{NLI} from Line 2.1.

Line 2.3: The supplier margin provides allocation for normal product variations due to the manufacturing process, marine operations and environmental conditions as they pertain to $GSNR$.

Line 2.4: This is the system average $GSNR$ under flat launch conditions at BOL. Line 2.4 $GSNR$ is given by subtracting Line 2.3 from Line 2.2.

Line 2.5: Represents the penalty experienced by the average $GSNR$ due to the pre-emphasis based equalization performed to arrive at Line 1.7, relative to the average $GSNR$ under flat launch conditions.

Line 2.6: This represents the average $GSNR$ performance at BOL under the agreed equalized conditions per Line 1.7. It is the subtraction of Line 2.5 from Line 2.4. This value may be agreed as a commissioning target.

Line 2.7: This is the allowance for spectral variation of performance across the band. The values correspond to the worst case $GSNR$ across the band after equalization. This value may be agreed as a commissioning target.

Line 2.8: Represents the average $GSNR$ after agreed equalization has been applied under EOL conditions. The Line 2.8 $GSNR$ is calculated using the generalized signal droop formula using the Line 2.6, with the added SNR_{ASE} penalty due to aging and repairs, Line 1.10.

Line 2.9: This is the allowance for spectral variation of performance across the band. The values correspond to the worst case $GSNR$ across the band after agreed equalization under EOL conditions.

TABLE III
TTE OVER WET PLANT SNR BUDGET TABLE

	Segment Information	SNR [dB]	SNR Change [dB]
	Wet Plant		
1.1	SNR_{ASE}	12.9	
1.2	Nonlinearity	15.3	
	TTE		
2.1	Nonlinearity Improvement		0.2
2.2	Modem Implementation (SNR_m)	16.0	
2.3	Other Impairments (SNR_i)	24.5	
2.4	TTE Required (SNR_{TOT}^{b2b})	8.0	
	TTE and Wet Plant		
3.1	Time Varying System Penalty (TVSP)		0.1
3.2	Total SNR (SNR_{TOT})	9.6	
	Margin		
4.1	Customer SNR Margin		0.5
4.2	Required System SNR	8.6	
4.3	Net System Margin	1.0	

C. SNR Budget Table for TTE Over Wet Plant

In this section we propose Table III , which can be used to define SNR performance margins that can be achieved with a particular vendor and mode of operation of TTE technology, utilizing the SNR-based performance metrics specified in Table II. While a traditional Q-based budget table can still be generated from the same metrics, we believe an SNR-based TTE performance budget better represents the SNR margin available for conversion into fiber and cable capacity.

The information required from Table II should be passed on by the system owner to the TTE vendor for use in producing this table. The table can be generated both before and after the characterization of the wet plant, using either pre-construction design parameters or post-commissioning detailed data. The wet plant parameters used should be selected in accordance to the owners' preferences, risk tolerances and available information. A risk-adverse owner may provide the worst case commissioning values to receive an estimate of the minimum capacity expected during the design phase. Others may prefer capacity estimations be performed assuming not all of the supplier margin in Table II is consumed, using SNR values higher than the commissioning values. The wet plant values provided to the TTE vendor can also be the measured values, as collected during the system commissioning, if that phase of the project is completed. In this case, the cable owner can provide the measured

TABLE IV
ACRONYM LIST

SNR	Signal to Noise Ratio
GSNR	Gaussian or Generalized SNR
ASE	Amplified Spontaneous Emission
GAWBS	Guided Acoustic Wave Brillouin Scattering
Q or Q^2	Quality
OSNR	Optical SNR
GOSNR	Gaussian or Generalized Optical SNR
QPSK	Quaternary Phase Shift Keying
SDM	Spatial Division Multiplexing
EDFA	Erbium Doped Fiber Amplifier
ROADM	Reconfigurable Optical Add Drop Multiplexer
TOP	Total Output Power
NLI	NonLinearities
AWGN	Additive White Gaussian Noise
GN	Gaussian Noise
PSD	Power Spectral Density
SPM	Self Phase Modulation
XPM	Cross Phase Modulation
Aeff	Effective Area
OCI	Open Cable Interface
TTE	Terminal Transmission Equipment
PDL	Polarization Dependent Loss
PMD	Polarization Mode Dispersion
LO	Local Oscillator
Tx	Transmitter
Rx	Receiver
WDM	Wavelength Division Multiplexing
SHB	Spectral Hole Burning
MUX	Multiplexer
SNREQ	SNRASE EQualized
PFIB	Fiber power equalized
NLC	NonLinear Compensation
CD (C)	Chromatic Dispersion (Compensation)
RRC	Root Raised Cosine
DSP	Digital Signal Processing
DEMUX	Demultiplexer
QAM	Quaternary Amplitude Modulation
FEC	Forward Error Code
PE	Pre-Emphasis
BPSK	Binary Phase Shift Keying
BER	Bit Error Rate
FP	Fiber Pair
LEAF	Large Effective Area Fiber
DSF	Dispersion Shifted Fiber
KPT	Key Parameter Table
BOL	Beginning Of Life
EOL	End Of Life
TVSP	Time Varying System Penalty
DLS	Digital Line Segment

frequency-dependent SNR performance data, as described in Section V-A for the most accurate capacity estimation prior to TTE deployment.

A line-by-line description of Table III is provided as follows:

Line 1.1: The SNR_{ASE} for the selected conditions of the budget table produced for the DLS. This may include but is not limited to Line 1.4 or Line 1.8 of Table II.

Line 1.2: The fiber nonlinearity as defined as the reciprocal sum of Line 2.0 and Line 2.1 of Table II.

Line 2.1: Any improvements by the TTE due to the nonlinearity stated in Line 1.2 should be added or subtracted here.

Line 2.2: The back-to-back implementation noise of the TTE.

Line 2.3: All other implementation noises due to propagation over the DLS. Examples of SNR_i are described in Section III-B.

Line 2.4: The back-to-back SNR_{TOT} specified at the FEC limit.

Line 3.1: The 5-sigma time-varying system penalty (TVSP) as predicted or measured by the TTE on the DLS.

Line 3.2: The inverse reciprocal sum of all SNR terms in Lines 1.1, 1.2, 2.2, and 2.3. Any nonlinear improvements from Line 2.1 should be considered accordingly.

Line 4.1: This line may include any additional operating margins requested by the customer.

Line 4.2: The minimum SNR_{TOT} for the DLS including the customer margin. It is the summation of Lines 2.4, 3.1 and 4.1.

Line 4.3: The final net system margin delivered by the TTE. It is the difference between the total TTE's Required SNR (Line 2.4) and the DLS' Total SNR (Line 4.2). Line 4.3 should be positive for error-free operation.

VI. Conclusion

This paper summarizes a cross-industry collaboration aiming to consolidate the basic definitions and procedures for the design, acceptance and capacity of subsea open cables. SNR definitions, including fiber nonlinearity, GAWBS and signal droop are introduced to comprehensively define the performance of subsea systems. Capacity metrics for open cables are introduced using the Shannon formulation as a vendor-agnostic framework. In addition, guidelines for the estimation of capacity with modern terminal equipment are proposed. Scaling rules to variants in channel planning or multi-segment transmission are explained. Finally, performance tables are proposed to define and commission subsea open cables. This work sets the basis for an efficient definition, deployment and operation of modern subsea networks that support the backbone of global connectivity now and in the years to come.

Acknowledgment

The authors deeply appreciate the discussions with Infinera and specifically Marc Stephens and Emilio Bravi who brought a complementary vision on how to manage the transponders in this paper.

The authors also acknowledge important perspectives from Telstra, with particular acknowledgment to Philip Murphy, Paul Lomas and Chris Mott.

References

[1] E. Grellier and A. Bononi, "Quality parameter for coherent transmissions with Gaussian-distributed nonlinear noise," *Opt. Exp.,* vol. 19, pp. 12781–12788, 2011.

[2] P. Poggiolini, A. Carena, V. Curri, G. Bosco, and F. Forghieri, "Analytical modeling of nonlinear propagation in uncompensated optical transmission links," *PTL*, vol. 23, no. 11, pp. 742–744, Jun. 2011.

[3] M. Enright, E. Muth, J. Thogoluva, and G. Mohs, "Open cables and interaction with terrestrial networks," in *Proc. SubOptic*, Dubai, UAE, 2016, Paper WE2A.4.

[4] V. Kamalov *et al.*, "Lessons learned from open line system deployments," in *Proc. Opt. Fiber Commun. Conf. Exhib.,* Los Angeles, CA, USA, 2017, Paper M2E.2.

[5] T. Stuch and J. Gaudette, "Open undersea cable systems for cloud scale operation," in *Proc. Opt. Fiber Commun. Conf. Exhib.*, Los Angeles, CA, USA, 2017, Paper M2E.1.

[6] E. Rivera Hartling, "From the acceptance of turnkey systems to open networks with G-SNR," in *Proc. Opt. Fiber Commun. Conf. Exhib.*, San Diego, CA, USA, 2020, Tutorial W1J.4.

[7] Neal S. Bergano, "Wavelength division multiplexing in long-haul transoceanic transmission systems," *J. Lightw. Technol.,* vol. 23, no. 12, Dec. 2005, Art. no. 4125.

[8] O. V. Sinkin *et al.*, "Effective signal to noise ratio performance metric for dispersion-uncompensated links," in *Proc. Eur. Conf. Opt. Commun.*, Valencia, Spain, 2015, Paper P.5.3.

[9] P. Pecci, S. Dupont, S. Dubost, S. Ruggeri, O. Courtois, and V. Letellier, "Experimental characterization of submarine "Open Cable" using Gaussian-noise model and OSNRWET parameter," in *Proc. Opt. Fiber Commun. Conf. Exhib.*, Los Angeles, CA, USA, 2017, Paper M2E.4.

[10] E. Mateo, K. Nakamura, T. Inoue, Y. Inada, and T. Ogata, "Nonlinear characterization of fiber optic submarine cables," in *Proc. Eur. Conf. Opt. Commun.*, Gothenburg, Sweden, 2017, Paper Th.2.E.4.

[11] A. Carbo Meseguer, P. Plantady, A. Calsat, S. Dubost, J.C. Antona, and V. Letellier, "Automated full c-band technique for fast characterization of subsea open cable G-SNR," in *Proc. Asia Commun. Photon. Conf.*, Chengdu, China, 2019, Paper S4B.5.

[12] E. Rivera Hartling *et al.*, "Subsea open cables: A practical perspective on the guidelines and gotchas," in *Proc. SubOptic*, New Orleans, LA, USA, 2019.

[13] A. Pilipetskii, "High capacity submarine transmission systems," in *Proc. Opt. Fiber Commun. Conf. Exhib.*, Los Angeles, CA, USA, 2015, Tutorial W3G.5.

[14] E. Mateo, Y. Inada, T. Ogata, S. Mikami, V. Kamalov, and V. Vusirikala, "Capacity limits of submarine cables," in *Proc. SubOptic*, Dubai, UAE, 2016, Paper TH1A.1.

[15] A. Pilipetskii, D. Foursa, M. Bolshtyansky, G. Mohs, and N. S. Bergano, "Optical designs for greater power efficiency," in *Proc. SubOptic*, Dubai, UAE, 2016, Paper TH1A.5.

[16] O. Domingues, D. Mello. S. Ö. Arik, and J. M. Kahn, "Capacity limits of space-division multiplexed submarine links subject to nonlinearities and power feed constraints," in *Proc. Opt. Fiber Commun. Conf. Exhib.*, Los Angeles, CA, USA, 2017, Paper Th2A.50.

[17] R. Dar *et al.*, "Submarine cable cost reduction through massive SDM," in *Proc. Eur. Conf. Opt. Commun.*, Gothenburg, Sweden, 2017, Paper Tu.1.E.5.

[18] J. Downie, "Maximum cable capacity in submarine systems with power feed constraints and implications for SDM requirements," in *Proc. Eur. Conf. Opt. Commun.*, Gothenburg, Sweden, 2017, Paper Tu.1.E.4.

[19] M. A. Bolshtyansky *et al.*, "Single-mode fiber SDM submarine systems," *J. Lightw. Technol*, vol. 38, no. 6, pp. 1296–1304, 2020.

[20] R.M. Shelby, M.D. Levenson, and P.W. Bayer, "Guided acoustic-wave Brillouin scattering," *Phys. Rev. B*, vol. 31, no. 8, pp. 5244–5252, 1985.

[21] M. A. Bolshtyansky *et al.*, "Impact of spontaneous guided acoustic-wave Brillouin scattering on long-haul transmission," in *Proc. Opt. Fiber Commun. Conf. Expo.*, San Diego, CA, USA, 2018, Paper M4B.3.

[22] M. Nakazawa, M. Yoshida, M. Terayama, S. Okamoto, K. Kasai, and T. Hirooka, "Observation of guided acoustic-wave Brillouin scattering noise and its compensation in digital coherent optical fiber transmission systems," *Opt. Exp.*, vol. 26, no. 7, 2018, Art. no. 9171.

[23] P. Serena, F. Poli, A. Bononi, and J.-C. Antona, "Scattering efficiency of thermally excited GAWBS in fibers for optical communications," in *Proc. Eur. Conf. Opt. Commun.*, Dublin, Ireland, 2019, Paper Tu1C2.

[24] M. Paskov, M. A. Bolshtyansky, J.-X. Cai, C. R. Davidson, D. G. Foursa, and A. N. Pilipetskii, "Observation and compensation of GAWBS in modulated channels," in *Proc. Opt. Fiber Commun. Conf. Exhib.*, San Diego, CA, USA, 2019, Paper Tu3J.3.
[25] J. C. Antona, A. Meseguer, and V. Letellier, "Transmission systems with constant output power amplifiers at Low SNR values: A generalized droop model," in *Proc. Opt. Fiber Commun. Conf. Exhib.*, San Diego, CA, USA, 2019, Paper M1J.6.
[26] Optical System Design and Engineering considerations, ITU-T, Series G, Supplement. vol. 39, Sep. 2012.
[27] J. Gaudette, E. Rivera Hartling, M. O'Sullivan, P. Booi, and M. Andre, "Using coherent technology for simple, accurate performance budgeting," in *Proc. SubOptic*, Paris, France, 2013, Paper WE.1A.02.
[28] P. Poggiolini, "The GN model of non-linear propagation in uncompensated coherent optical systems," *J. Lightw. Technol.*, vol. 30, no. 24, pp. 3857–3879, Dec. 2012.
[29] A. Bononi, J. C. Antona, M. Lonardi, A. Carbo-Meseguer, and P. Serena, "The generalized droop formula for low signal to noise ratio optical links," *J. Lightw. Technol.*, vol. 38, no. 8, pp. 2201–2213, 2020.
[30] L. E. Nelson, "Polarization effects in coherent systems," in *Proc. Opt. Fiber Commun. Conf. Exhib.*, Los Angeles, CA, USA, 2012, Paper OTu1A.4.
[31] "Characteristics of optically amplified optical fibre submarine cable systems," ITU-T, Series G, G.977, Jan. 2015.
[32] W. Shieh and K. Ho, "Equalization-enhanced phase noise for coherent detection systems using electronic digital signal processing," *Opt. Exp.*, vol. 16, no. 20, 2008, Art. no. 15718.
[33] G. He, S. Searcy, D. Gariépy and S. Tibuleac, "GOSNR characterization by optical spectrum analysis," in *Proc. Opt. Fiber Commun. Conf. Exhib.*, San Diego, CA, USA, 2020, Paper W2A.21.
[34] R. Ryf *et al.*, "White Gaussian noise based capacity estimate and characterization of fiber-optic link," in *Proc. Opt. Fiber Commun. Conf. Expo.*, San Diego, CA, USA, 2018, Paper W1G.2.
[35] A. D. Shiner *et al.*, "Neural network training for OSNR estimation from prototype to product," in *Proc. Opt. Fiber Commun. Conf. Expo.*, San Diego, CA, USA, 2020, Paper M4E.2.
[36] A. Kam *et al.*, "Pre-emphasis-based equalization strategy to maximize cable performance," in *Proc. SubOptic*, New Orleans, LA, USA, 2019, Paper OP14-1.
[37] V. Kamalov *et al.*, "The subsea fiber as a shannon channel," in *Proc. SubOptic*, New Orleans, LA, USA, 2019, Paper OP12-2.
[38] A. D. Ellis, M. E. McCarthy, M. A. Z. Al Khateeb, M. Sorokina, and N. J. Doran, "Performance limits in optical communications due to fiber nonlinearity," *Adv. Opt. Photon.*, vol. 9, no. 3, pp. 429–502, 2017.
[39] J. G. Proakis, *Digital Communications*. McGraw-Hill, 1995.
[40] J. R. Barry, E. A. Lee, D. G. Messerschmitt, *Digital Communications.* Springer, 2003.
[41] K. Roberts, Q. Zhuge, I. Monga, S. Gareau, and C. Laperle, "Beyond 100 Gb/s: Capacity, flexibility and network optimization," *J. Opt. Commun. Netw.*, vol. 9, no. 4, pp. C12–C24, 2017.
[42] M. Reimer, S. Oveis Gharan, A. D. Shiner, and M. O'Sullivan, "Optimized 4 and 8 dimensional modulation formats for variable capacity in optical networks," in *Proc. Opt. Fiber Commun. Conf. Expo.*, Anaheim, CA, USA, 2016, Paper M3A.4.
[43] M. C. Jeruchim, P. Balaban, and K. S. Shanmugan, *Simulation of Communication Systems.* Norwell, MA, USA: Kluwer Academic Publishers, 2002.

Elizabeth Rivera Hartling was born in Canada, in 1986. She received the B.Sc. degree in electrical engineering from Queen's University, Kingston, Ontario, Canada, in 2008. She joined Nortel Networks in 2008 as a Founding Member of the Submarine R&D engineering team, continuing this work within Ciena following the acquisition of the Metro Ethernet Networks division of Nortel Networks by Ciena in 2010. In this role, she designed and executed solutions for some of the very first subsea industry 40G and 100G coherent upgrades and co-pioneered the ITU standardization of submarine power budget tables for coherent technologies. She contributed to a chapter entitled "Submarine cable upgrades" in the text "Undersea Fiber Communication Systems" edited by José Chesnoy. She joined Facebook in 2018 as a Subsea Optical Network Architect, focusing on optical transmission technology and optimizing Facebook's subsea Open Cable designs to build a scalable, high capacity, cost-effective global subsea network. She has been a long-time champion of the subsea Open Cables movement and in her current role with Facebook recently led a cross-industry working group focused on garnering broad industry agreement on best practices and recommendations for many key aspects of Open Cables.

Alexei Pilipetskii was born in Russia, Moscow, in 1962. He received the M.S. degree in physics from Moscow State University in 1985. He received the Ph.D. degree in 1990 from General Physics Institute, Academy of Sciences Russia, for the research in nonlinear fiber optics. From 1994 to 1997, he was at the University of Maryland, Baltimore County, where his interests shifted to the fiber optic data transmission. In 1997, he joined AT&T Submarine Systems, currently SubCom. Alexei is the Leader of the Forward Looking Team focused on the transmission research and introduction of the new technologies. Alexei is a IEEE Photonics Society Fellow.

Darwin Evans was born in Manitoba, Canada, in 1975. He received the B.S. degree in computer engineering from the University of Manitoba in 1998. From 1999 to 2010, he worked on a number of engineering and product development roles with Nortel Networks until the acquisition of the Nortel Metro Ethernet Networks division by Ciena in 2010. Since 2015, he has been the Product Line Manager responsible for submarine applications at Ciena.

Eduardo Mateo was born in Madrid, Spain. He received the Ph.D. degree in physics from the University of Santiago de Compostela, Spain, in 2005 in the field of Integrated Nonlinear Optics. He was a Research Scientist with CREOL (Orlando, FL) conducting pioneering research in nonlinear fiber optics, optical fiber communications, and digital signal processing. In 2009, he joined NEC Laboratories America (Princeton NJ, USA), where he conducted research activities on ultra-long haul fiber transmission and large capacity systems. In 2012, he joined the Submarine Network Division in NEC headquarters (Tokyo, Japan) where he is currently the Director of Network Architecture and Core Technology Strategy. He has authored and coauthored more than 80 publications and patents including a book chapter in submarine networks.

Massimiliano Salsi (Member, IEEE) was born in Parma, Italy, in 1979. He received the Laurea degree in telecommunication engineering (*cum laude*) and the Ph.D. degree in information technology from the University of Parma, in 2004 and 2008, respectively. Between 2008 and 2014, he was a member of the technical staff with Bell Labs, France, where he worked on submarine technologies, system design, signal processing for coherent transponders, and some pioneering experiments on mode division multiplexing. In 2014, he joined Juniper Networks' Development and Innovation department with the goal of integrating WDM optical technology into IP devices. Since 2018, he has been a network architect with Google, responsible for its global submarine network infrastructure. Dr. Salsi has authored or coauthored more than 50 papers and 30 patent applications.

Pascal Pecci was born in France in a city close to the Luxembourg border, in 1972. After the Ph.D. degree in 2000, Pascal Pecci started working for Alcatel Research and Innovation on 40G transmission in optical fiber and had two world records transmission. After nine years in R&D he joined the Product Line Management team to become a PLM of the Alcatel Lucent design tools for terrestrial networks. In 2013, Pascal Pecci joined the Submarine division of Alcatel-Lucent, where he defined the design rules for submarine and designed many advanced networks on Atlantic and Pacific oceans. He wrote a chapter entitled "ULH submarine transmission" in "Undersea Fiber communication systems" book edited by José Chesnoy and had articles in recent Suboptic, OFC, and ECOC. In 2018, he joined submarine PLM team of ASN. In 2019, he was promoted to SDM_1 by ASN solution.

Priyanth Mehta is a Hardware Engineer for the Optical Systems Performance team with Ciena in Ottawa, Canada. He received the B.Sc. (Hons.) degree in 2007 and the M.Sc. (Hons.) degree in 2009, in optical physics from the University of Auckland, New Zealand. He then received the Ph.D. degree in nonlinear optics from the Optoelectronics Research Centre, University of Southampton, U.K., in 2013. Priyanth's primary fields of research at Ciena are focussed on improving transmission capacity, reach, and user operability through modem and line terminal enhancements. Priyanth also is a contributing delegate and Editor in Standardization on the International Telecommunication Union (ITU) for Optical Transport and Access.